ISBN: 978-3-95450-240-0 ISSN: 2673-5539 doi:10.18429/JACoW-RuPAC2021-WEPSC15

BARRIER STATION RF1 OF THE NICA COLLIDER. DESIGN FEATURES AND INFLUENCE ON BEAM DYNAMICS

A.M. Malyshev, A.A. Krasnov, Ya.G. Kruchkov, S.A. Krutikhin, G.Y. Kurkin, A.Yu. Martynovsky, N.V. Mityanina[1], S.V. Motygin, A.A. Murasev[1], V.N. Osipov, V.M. Petrov, A.M. Pilan[2], E. Rotov[1], V.V. Tarnetsky[1], A.G. Tribendis[2], I.A. Zapryagaev[1], A.A. Zhukov, Budker INP, Novosibirsk, Russia
O.I. Brovko, I.N. Meshkov[3], E. M. Syresin, JINR, Dubna, Russia
[1]also at Novosibirsk State University, Novosibirsk, Russia
[2]also at Novosibirsk State Technical University, Novosibirsk, Russia
[3]also at Saint-Petersburg State University, Saint-Petersburg, Russia

Abstract

This paper reports on the design features and construction progress of the barrier bucket RF systems for the NICA collider being built at JINR, Dubna. Each of two collider rings has three RF systems named RF1 to 3. RF1 is a barrier bucket system used for particles capturing and accumulation during injection, RF2 and 3 are resonant systems operating at 22nd and 66th harmonics of the revolution frequency and used for the 22 bunches formation. The RF systems are designed by Budker INP. Both RF1 stations were manufactured, delivered to JINR and tested at the stand. The test results are presented in the article, as well as some results of calculating the effect of the RF1 system on the beam dynamics.

INTRODUCTION

The Nuclotron based Ion Collider fAcility (NICA) [1], operating in its heavy ion collision mode is aimed at the experiments with colliding beams of $^{197}Au^{79+}$ ions at energies from 1 to 4.5 GeV/u per beam. Budker Institute of Nuclear Physics contributes to several parts of the project, including its RF systems – barrier bucket and harmonic. Barrier bucket system, RF1, is used to capture the particles injected from the Nuclotron and to accumulate the required number of ions. This is done using moving barriers technique. RF1 also can accelerate the accumulated beam if the injection energy is lower than that of the experiment. Harmonic systems, RF2 and 3, are used to form 22 bunches with required parameters. Each collider ring has one RF1 station, four RF2 and eight RF3 stations.

The RF1 system generates 2 pairs of ±5 kV pulses (accelerating and decelerating in each pair) at the bunch revolution frequency thus forming the two separatrices – injection and stack. A bunch from the Nuclotron is shot into the injection separatrix, moved and added to the stack by switching off the pulses separating the two separatrices and so merging the two bunches. If the combined bunch length exceeds the half-ring perimeter it is compressed by moving the barrier pulses. Ion accumulation process is accomplished by the electron cooling. The accumulated ions trapped between the two barrier pulses may be accelerated, if needed, by ±0.3 kV meander voltage generated by the RF1 as well [2].

RF1 BARRIER BUCKET SYSTEM – INDUCTION ACCELERATOR

The barrier station is a coaxial line filled with 84XB-M grade amorphous iron rings. Pulse voltages generated by transistors operating in a switching mode are applied to the rings. These voltages are summed up at the accelerating gap of the station.

The station is cooled by water. There are channels for water flow between the rings of amorphous iron. Figure 1 shows the details of the RF1 station.

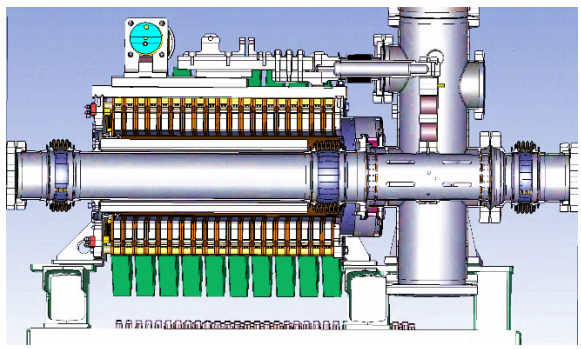

Figure 1: Details of the RF1 station.

To form the barrier voltage, 16 sections 6-20 are used, 3 accelerating sections 5-3, and one damping section.

At the moment when RF1 does not work, the accelerating gap is short-circuited by a contactor.

Figure 2 shows the appearance of the RF1 station.

Figure 2: Appearance of the RF1 station.

† alexmal94@mail.ru

ISBN: 978-3-95450-240-0 ISSN: 2673-5539 doi:10.18429/JACoW-RuPAC2021-WEPSC15

Stacking Algorithm

During injection of particles into the collider ring, particles are accumulated between the first and second pulses. In the interval between the third and fourth pulses, particles are injected. After the second and third pulses are turned off after their contraction, the accumulated bunch and the injected bunch are combined. The fourth voltage pulse becomes the second. Then it is necessary to switch on the third and fourth impulses accordingly in order to return to the initial location. The duration of the barrier voltage pulse can be adjusted from 80 ns to 10 ns.

If it is necessary to increase the energy, the accelerating voltage is switched on and at the same time, the magnetic field in the collider ring rises. Accelerating voltage (blue solid line on Fig. 3) - meander (0-300) V.

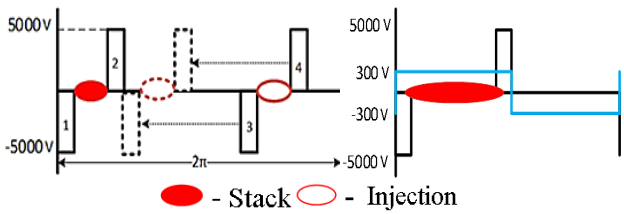

Figure 3: Barrier voltage (left) and acceleration (right).

TEST RESULTS OF RF1 STATION

Full load tests were carried out at a water temperature of + 30 ° C, a pressure drop (inlet-outlet) of 3.5 atm. and flow rate ~ 70 l / min. The maximum temperature in the pulse generators was + 47 ° C. The maximum temperature in amorphous iron was + 33 ° C. The heating protection threshold for output transistors is set at +60 ºC.

The operability of the power supplies of the accelerating and barrier sections for the equivalent and as part of the station has been checked. The accuracy of the output voltage is +/- 1%.

Oscillograms of the accelerating and barrier voltages were obtained, see Fig. 4, Fig 5.

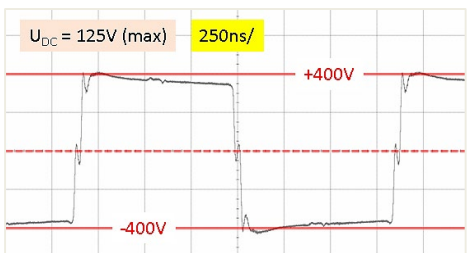

Figure 4: Accelerating voltage of RF1 station.

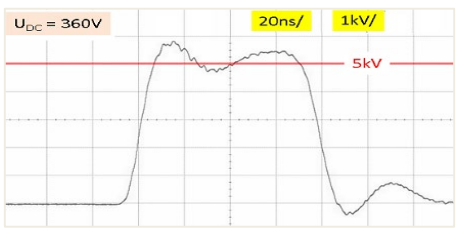

Figure 5: Barrier voltage of RF1 station.

INFLUENCE OF THE BARRIER SYSTEM ON BEAM DYNAMICS

Figure 6 shows a sketch of the entire RF1 station and a diagram of the connection of the RF1 station rings to the accelerating gap with rectangular voltage sources.

On equivalent circuits (Fig. 6, Fig. 7, Fig. 8) numbers 1-6 indicate parts of the rings: 1 – key (pulse generator); 2 - primary loop (from pulse generator to amorphous iron); 3 - amorphous iron; 4 - secondary loop (parasitic gap around the inductor); 5 - coaxial; 6 - accelerating gap.

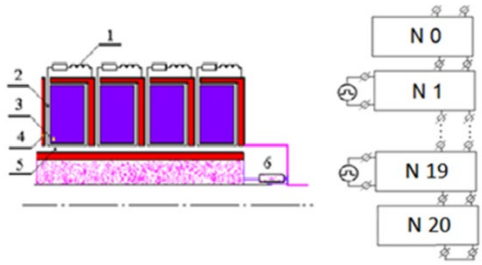

Figure 6: Connection of the RF1 station rings to the accelerating gap.

3D modeling of the RF1 station is impossible due to the complexity of the design, since it is necessary to take into account not only geometric, but also electrical parameters.

Therefore, the simulation of output voltage and impedance were carried out using equivalent circuits on Fig. 7, Fig.8. Figure 7 shows the equivalent circuit one ring for the rings with numbers N=1-19.

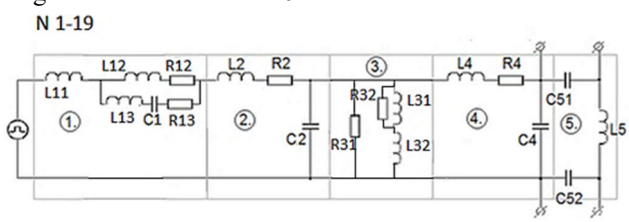

Figure 7: Equivalent circuit of one ring (from the 1st to the 19th).

Circuit of the last ring (N20) and accelerating gap (N0) are shown in Fig. 8.

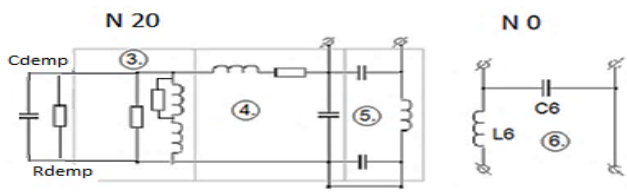

Figure 8: Last ring and accelerating gap.

The measurements of the station and calculations of its model with the estimated parameters were carried out.

Using the equivalent circuit, the signal transmission through the structure (Fig. 9) and the impedance (Fig. 10) are calculated.

Parameters of equivalent circuit are estimated with independent inductances and capacitances (quasistatic approach) and corrected so that simulation of output voltage was in sufficient accordance with measured one (Fig. 9).

ISBN: 978-3-95450-240-0 ISSN: 2673-5539 doi:10.18429/JACoW-RuPAC2021-WEPSC15

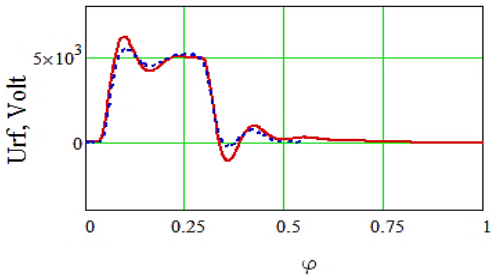

Figure 9: Comparison of measured (blue dash-dotted line) and calculated (solid red line) output pulse.

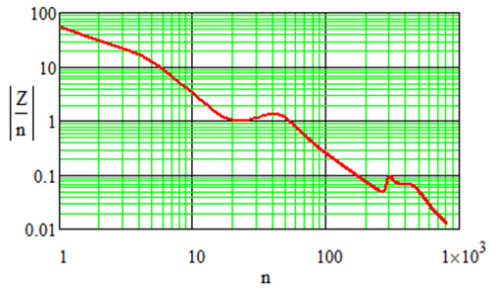

Figure 10: System impedance calculated by equivalent circuit impedance, Z_{out}/n.

The RF voltage affecting the particle dynamics includes the RF system output voltage Urf (obtained above, Fig. 9), the beam-induced voltage Uind, taking into account the output impedance of the station RF1 and the harmonics of the beam longitudinal distribution function, and the space charge field voltage, proportional to this distribution function:

$$U(\varphi) = U_{rf}(\varphi) + U_{sc}(\varphi,\rho) + U_{ind}(\varphi,\rho)$$

The beam particles undergo phase motion in the potential of this voltage:

$$W(\Delta\varphi) = k_0 \frac{Z_{Au}}{A_{Au}} e \int_0^{\Delta\varphi} (U(\varphi_s + \Delta\varphi) - U(\varphi_s)) d\varphi$$

$$k_0 = \frac{q_{rf}}{2\pi} \frac{\omega_0 \eta}{R_s p_s} > 0, \qquad \eta = \gamma_s^{-2} - \alpha$$

The stationary (Boltzmann) distribution is defined with account of the total potential:

$$\rho(\varphi) = C \cdot \exp\left(-\frac{W_{rf}(\varphi) + W_{sc}(\varphi,\rho) + W_{ind}(\varphi,\rho)}{\delta_{p\,av}{}^2 (\omega_0 \eta)^2} \right)$$

$$\int_0^{2\pi} \rho(\varphi) d\varphi = Q = I_0 / f_0, \quad \delta_{p\,av}{}^2 = \left\langle (\Delta p / p_s)^2 \right\rangle$$

The (self-consistent) longitudinal distribution is found by solving the self-consistent problem by iterations (Fig. 11), in which the initial approximation is calculated without taking into account the induced voltage and the space charge field (black dash-dotted line on Fig. 11).

As a result, with the maximum possible spread of longitudinal pulses, we obtain a longitudinal distribution and the shape of a potential well at a beam current of 0.4 A. and an ion energy of 3 GeV/u. These calculations shows that the stationary longitudinal distribution of the beam 0.4A can exist.

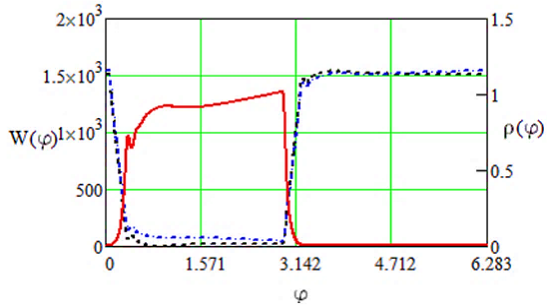

Figure 11: Longitudinal distribution (solid red line); RF potential - black dash-dotted line; total Self-Consistent Potential - blue dash-dotted line.

Microwave Instability

A table of threshold values of the beam current at energies from 1 to 4.5 GeV/u was calculated (Table 1, φbb = 10/12π).

$$I_0 \le \varphi_{bb} \frac{(A_{Au} E / Z_{Au} e) |\eta| \delta_{p\,av}{}^2}{|Z_{out}(n\omega_0)/n|_{\max}}$$

RF1 impedance (max 60ohm, see Fig. 10) at 0.4A does not cause microwave instability.

Table 1: Microwave Instability Threshold

Energy, GeV/u	**1**	**3**	**4.5**
$\Delta p_{sep}/3$, 10^{-3}	0.24	0.37	0.6
Threshold current, A, at $\lvert Z/n\rvert_{\max} = 60\ Ohm$	2.6A	2.2A	0.8A

CONCLUSION

The results of testing the station at the stand are obtained.

An equivalent circuit diagram of the station was compiled, taking into account the design features and measurements of the finished station. The parameters of the station were measured and simulations were carried out.

The calculations of the beam dynamics have been carried out, which show that the stationary longitudinal distribution of the beam 0.4A can exist and no microwave instability arises during the operation of the station.

REFERENCES

[1] D. Kekelidze *et al.*, "Three stages of the NICA accelerator complex", *Eur. Phys. J.* A (2016) 52: 211. doi:10.1140/epja/i2016-16211-2

[2] A. G. Tribendis *et al.*, "Construction and First Test Results of the Barrier and Harmonic RF Systems for the NICA Collider", presented at the *12th Int. Particle Accelerator Conf. (IPAC'21)*, Campinas, Brazil, May 2021, paper MOPAB365.